J. Phys. IV France **134** (2006) 257–262

DOI: 10.1051/jp4:2006134039

Equation of state and elastic properties of beryllium from first principles calculations

G. Robert[1] and A. Sollier[1]

[1] *CEA-DIF, BP. 12, 91680 Bruyères-le-Châtel, France*

Abstract. The electronic and structural properties of beryllium were investigated under high pressure using first principle pseudopotential calculations within the generalized gradient approximation (GGA). Our results including pressures, elastic constants, Debye temperatures for two crystal structures (α hexagonal close packed and β body-centred cubic) are compared with the experimental and other theoretical data over a wide density range. Calculated phonon spectra allow us to explain the anomalous behavior of the hcp-bcc transition under pressure. An equation of state (EOS) for the hcp phase at finite temperatures is derived taking into account the anharmonicity effects of thermal lattice vibrations. The resulting 300 K isotherm and Hugoniot curve, as well as the evolution of the shear modulus under pressure and temperature, are in good agreement with available experimental and theoretical data.

1. INTRODUCTION

Beryllium (Be) has long been the subject of a great deal of interest from the scientific community because of its simple atomic configuration and unusual physical properties. It is characterized by excellent structural properties (high strength, high melting point) in addition to unique radiation characteristics (transparent to X-ray, high neutron reflector).

Under ambient conditions Be metal has a α hexagonal close packed (hcp) structure with two atoms/cell and with only two valence electrons per atom. This crystal structure is non-ideal as the axial ratio $c/a = 1.568$ at room pressure significantly differs from the ideal close-packed value of 1.633. Be is also characterized by a very small Poisson ratio ($\nu(\rho_0) \approx 0.04$). All these anomalous properties are attributed to deviations from simple nearly free electrons behavior [1]. The experimental phase diagram of Be (Figure 1) is only known, under pressure, below 6 GPa [2]. At 1530 K, Be transforms into a β body-centred cubic (bcc) structure, which melts at 1550 K. The decrease of the $\alpha - \beta$ transition temperature under compression suggests a possible hcp to bcc transition at ambient temperature under high pressures. While earlier experimental data [3] found such a phase transition above 180 GPa, recent x-ray diffraction results [4][5] failed to find it. Theoretical high-pressure studies [6][7] found the $\alpha - \beta$ transition around 200 GPa. The negative slope at low pressure could also indicate a mechanically unstable behavior of the bcc structure [7]. The Debye temperature Θ_D is high and shows a strong dependence as a function of temperature. It decreases from 1440 K at a temperature of 4 K [8] to 925 K at ambient temperature [9]. These differences are of great importance in order to evaluate zero-point contribution to the total energy and phase transitions [6][7].

In this work, we have coupled density functional theory (DFT) with a Debye quasi-harmonic model in order to obtain the equation of state and the elastic properties of beryllium over a broad range of pressures and temperatures.

2. DETAILS OF CALCULATIONS

In the framework of DFT, the results are almost unchanged by the numerical approach used for the calculation (Full-Potential Linarized-Augmented-Plane-Wave, Projected Augmented Wave (PAW) or a Goedecker-Teter-Hutter (GTH) norm-conservative pseudopotentials) [10]. Our calculations have been performed within the Generalized Gradient Approximation (GGA) [11]. As a preliminary step, we have

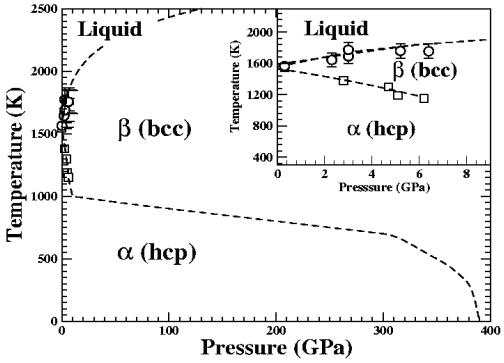

Figure 1. Phase diagram of beryllium. Circles and squares come from experimental data [2]. Dashed lines draw an hyptothetical extension of the phase diagram

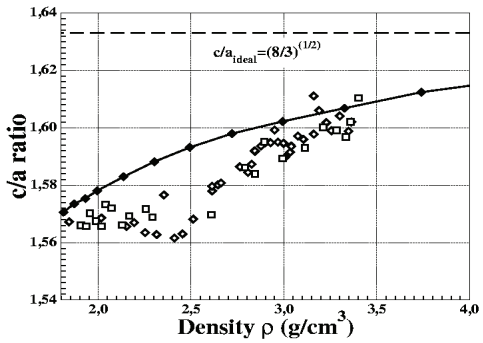

Figure 2. Calculated c/a axial ratio as a function of density for hcp Be (solid line with diamonds) compared with experimental data: □ [4] and ◇ [5]. Dashed line reproduces the ideal c/a ratio.

computed the structural and elastic constants using ***VASP*** code [12] with a PAW pseudopotential, which includes 4 electrons with a cut-off energy of 231.6 eV. The reciprocal space sampling was performed with a $24 \times 24 \times 24$ k-point mesh using a Gaussian smearing approach ($\sigma = 0.1$ eV). Unfortunately, linear response with PAW pseudopotentials is not yet implemented in this code. Phonon dispersions calculations of bulk Be are thus calculated with the ***abinit*** code [13] using linear response and a norm-conservative GTH pseudopotential which includes 4 electrons [14]. Our basis set included plane-waves up to a kinetic energy cut-off of 2200 eV. The reciprocal space sampling was performed with a $16 \times 16 \times 16$ k-point mesh for cubic structure, and a $12 \times 12 \times 12$ k-point mesh for hexagonal structure. For the phonons dispersion relations, we used 14 and 16 perturbations for bcc, and hcp phases respectively. For hcp phase, the optimisation of the c/a ratio is done for each volume.

3. PROPERTIES OF BERYLLIUM IN THE GROUND STATE

3.1 Elastic properties of hcp and bcc structures

The evolution of the c/a ratio as a function of density is reported in Figure 2. The calculated axial c/a ratios are in good agreement with experimental measurements [4][5] and previous theoretical calculations [7]. The electronic structure shows a dip near the Fermi level induced by the hybridisation between s and p valence bands. This effect coupled with an anisotropy between p_x (or p_y) and p_z bands character at 4 eV under the Fermi level can explain the unusual c/a ratio. When the c/a ratio tends towards its ideal value for an isochor or under compression, p_x (or p_y) states become degenerate with p_z bands character. These results, not show here, are in agreement with other theoretical results [7][15]. These electronic densities of states, combined with a Sommerfeld model will be used to take into account the thermal electronic excitations.

Elastic constants under pressure P were calculated using the method described in [16]. In order to evaluate the influence of homogeneous deformations on the values of the elastic constants, we used 8 different strains for the calculation of the five independent elastic constants c_{ij} of the hcp structure, and 6 different strains for the calculation of the three c_{ij} of the bcc cubic phase. The choice of different deformations for the calculation of a given elastic constant c_{ij} induces errors, which are around 5 % for c_{13} and c_{33}. For all other elastic constants values, the discrepancies are less than 1 %.

In order to extrapolate the elastic constants values at high compression, we choose an analytic formulation for $c_{ij}(\rho)$ similar to the one used in [17] to represent the evolution of the shear modulus

Table 1. Numerical values of the model parameters for hcp structure (left) and bcc structure (right).

	G_{VRH}	K_{VRH}	c_{11}	c_{12}	c_{13}	c_{33}	c_{44}	G_{VRH}	K_{VRH}	c_{11}	c_{12}	c_{44}
$c_{ij}(\rho_0)$	152,4	114,5	305,9	18,8	10,4	329	159,3	73,7	112,8	143,7	96,0	150,5
γ_1	0,199	0,876	0,658	1,247	1,116	0,599	-0,036	0	0,906	0,803	1,014	0,234
γ_2	2,109	5,517	8,044	158,739	25,355	2,836	1,246	4,107	66,811	212,828	−0,078	18,890
q	3,952	5,019	7,600	6,381	3,609	4,317	3,043	2,095	8,766	8,938	1,000	4,806
$c_{ij}(\rho_0)$ **[7]**	154,5	112,8	300,8	14,1	7,1	359,5	160,2	89,7	109,5	146,8	90,8	185,2
$c_{ij}(\rho_0)$ **[19]**	150,1	116,8	293,6	26,8	14,0	356,7	162,2					

with the density:

$$c_{ij}(\rho) = c_{ij}(\rho_0)\left(\frac{\rho}{\rho_0}\right)^{4/3} e^{[6\gamma_1(\rho_0^{-1/3}-\rho^{-1/3})+2\frac{\gamma_2}{q}(\rho_0^{-q}-\rho^{-q})]} \quad (1)$$

where ρ is the density (g/cm^3), ρ_0 is the experimental equilibrium density (1.8407 g/cm^3), $c_{ij}(\rho_0)$ (in GPa) are the elastic constants at equilibrium density. The values of free parameters γ_1, γ_2 and q for hcp and bcc structures are given in Table 1. With this analytic representation, the differences with the exact calculated values of c_{ij} are less than 0.2 % under compression. We can also use equation (1) in order to calculate bulk K and shear moduli G (see Table 1) with the same accuracy using the Voigt-Reuss-Hill averages: $G_{VRH} = (G_V + G_R)$ and $K_{VRH} = (K_V + K_R)$ where subscripts V and R point out Voigt and Reuss bounds respectively [18]. Our calculations of the elastic constants at equilibrium density $c_{ij}(\rho_0)$ are in good agreement with recent experimental data [19] and other theoretical calculations [7].

The analytic formulation of the elastic constant can be used to calculate the Poisson coefficient $\nu(\rho)$ and to obtain information on elastic anisotropy through the parameter $A_{VRH} = (G_V - G_R/(G_V + G_R)$. As we can see, the elastic properties are very different for the two structures. $A_{VRH}(\rho)$ is close to zero for hcp phase whereas it evolves from 0.7 at $\rho_0$to 0.2 at $\rho/\rho_0 \approx 3$ for bcc structure. For hcp phase, the Poisson coefficient at equilibrium density $\nu(\rho_0)$ is 0.04 (experimental values are typically between 0.02 and 0.06), and it is close to 1/3 for bcc phase. For both structures, $\nu(\rho)$ tends towards 1/3 under high compression. Elastic constants also show us that under a density of 1.62 g/cm^3, bcc phase is mechanically unstable against shear (the stability requirements c_{11}>c_{12} is not obeyed).

3.2 Phonon spectra of hcp and bcc structures

In order to obtain more information on stabilization effects and to build accurate thermal excitation of ions for our equation of state, we calculated phonon dispersions relations of bulk beryllium for the two structures. In Figure 3 we display the calculated phonon dispersions of bulk hcp Be and compare them with neutron diffraction data [20]. The overall agreement is very good and the discrepancy between our calculations and experimental values is less than 2-3 %. These calculations were carried out for ten densities ranging from $\rho/\rho_0 \approx 0.65$ up to $\rho/\rho_0 \approx 2$. For this range of density, hcp phase is always stable. As we can see on Figure 4, bcc structure exhibits a completely different behavior. Our calculations and other theoretical studies on elastic constants [7] show that bcc phase of beryllium become mechanically unstable for density under 1.62 g/cm^3 (Born condition $c_{11} > c_{12}$ is violated). But for density less than 2.0 g/cm^3, the frequency of N point phonon of the T1 branch in the [110] direction is already imaginary. This direction corresponds, for small displacements, to the elastic constant $(c_{11} - c_{12})/2$. If the density decreases under 1.65 g/cm^3, another unusual low frequency of the 2/3[111] transverse mode appears. This type of behavior indicates a possible martensitic transition before destabilization due to c_{ij}. As for zirconium, a stabilization of bcc phase in temperature due to strong anharmonic effects would occur. The stabilization of bcc phase (bcc becomes stable for a density of 1.80 g/cm^3 at 1530 K) and the negative slope of the hcp-bcc boundary at low pressure can be explained by two main coupling effects. First, for ρ between 1.8 and 2.0 g/cm^3, existence of soft phonons modes implies small recalling force, which creates a large entropy term [6]. So bcc phase is energetically more stable than hcp structure but mechanically

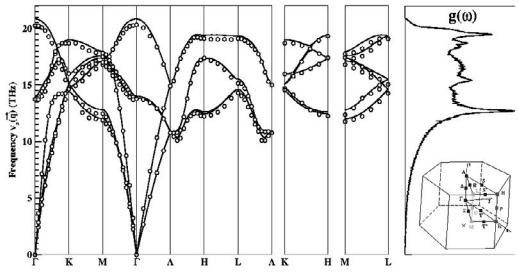

Figure 3. Phonon dispersions for hcp Be from our calculations at $\rho = 1.87$ g/cm^3 (lines) compared with neutron scattering data at 80K from Stedman *et al.* [20] (circles).

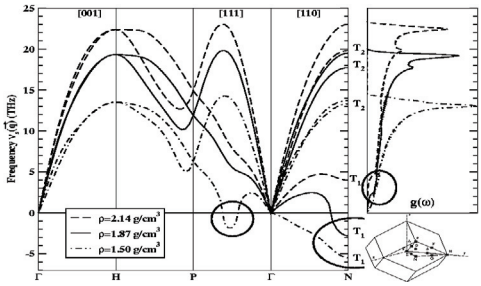

Figure 4. Calculated phonon dispersions for bcc Be in function of density. Circles point out soft phonons modes.

unstable. Stabilization is performed by thermal effects, which convert imaginary frequencies into small but real frequencies. Under pressure, soft phonons modes vanish and so does the negative slope of the hcp-bcc boundary (lower dashed line in Figure 1).

The knowledge of the phonon dispersions curves allows us to evaluate the Debye temperature $\Theta_D(n)$ as a function of moment frequencies n [18]. Each n moment frequency can be relied to a certain thermophysical property. For $n = -3$, Debye temperature corresponds to the elastic limit and low temperature properties. For $n = 0$, 1 and 2 it describes entropy, zero point energy correction and vibrationnal free energy respectively. Our calculations give $\Theta_D(-3) = 1475$ K (962 K) and $\Theta_D(2) = 930$ K (892 K) for hcp (bcc) structure, in very good agreement with the *ab initio* calculation of Sin'ko and Smirnov ($\Theta_D(-3) = 1465.9$ K) [7] from elastic constants, and the experimental value ($\Theta_D = 925$ K) of Hunderi and Myers [9] at ambient temperature. Using the same approach, we obtain a Grüneisen parameter of 1.3 for hcp phase, very close to the experimental estimation of 1.2 [19].

4. EQUATION OF STATE FOR HCP BERYLLIUM

An equation of state (EOS) for the hcp phase at finite temperatures is derived taking into account the anharmonicity effects of thermal lattice vibrations calculated using the Debye model with these $\Theta_D(n)$ [18]. The free energy due to the thermal excitations of electrons is also taken into account (see above). From $\Theta_D(1)$, we estimate the hcp-bcc phase transition around 390 GPa at 0K, which is higher than the estimation of Sin'ko and Smirnov equal to 270 GPa [7]. Previous calculations of elastic constants (Tables 1) allow us to obtain the Poisson coefficient as a function of volume. Assuming that this coefficient is constant for a given volume (ν((,T)= ((()), we can thus calculate the evolution of the shear modulus under pressure and temperature using the bulk modulus derived from our equation of state.

We first calculated the 300 K isotherm for hcp Be. It is shown in Figure 5 along with experimental data from static experiments [4][5] and theoretical predictions from the SESAME Be EOS [21]. We can see that our calculations are in very good agreement with the measurements of Evans et al. [5] as well as with the theoretical predictions of the SESAME EOS [21]. The measurements of Nakano et al. [4] are substantially stiffer than those of the other experimental studies. This is probably due to the fact that Nakano et al. [4] did not used any hydrostatic medium in their experiments, so that they measured the pressure in a nonhydrostatic sample with pressure gradient, whereas Evans et al. [5] used helium in their experiments. The others static properties, like equilibrium volume, c/a ratio (Figure 2), heat capacity, Poisson coefficient or elastic properties for a 1 bar isobar are also in good agreement with experimental results [10].

Using the Rankine-Hugoniot relations with our EOS, we have calculated the principle Hugoniot of hcp Be for pressures up to 100 GPa. Our high pressure shock Hugoniot data are shown (full lines)

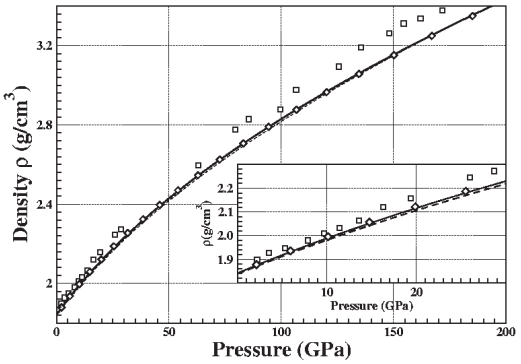

Figure 5. The calculated 300 K isotherm (solid line) for hcp Be compared with SESAME EOS (dashed line) [21] and experimental data : ([4]) and ([5]).

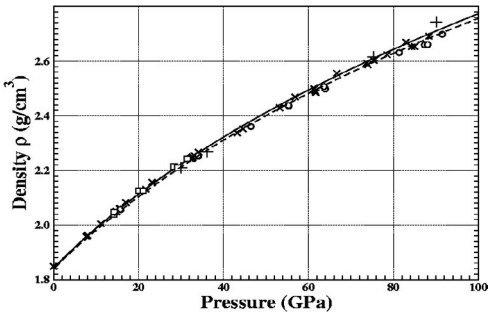

Figure 6. The calculated P-ρ curve for hcp Be under shock compression compared with SESAME EOS and various experimental data (see text).

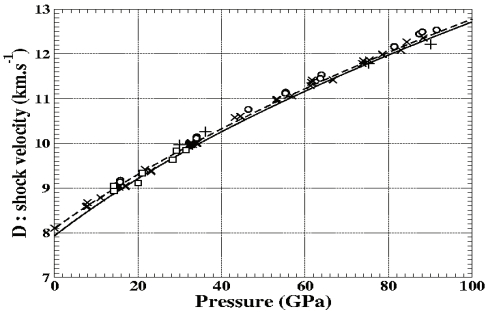

Figure 7. Calculated shock velocity D as a function of pressure P compared with SESAME EOS and various experimental data (see text).

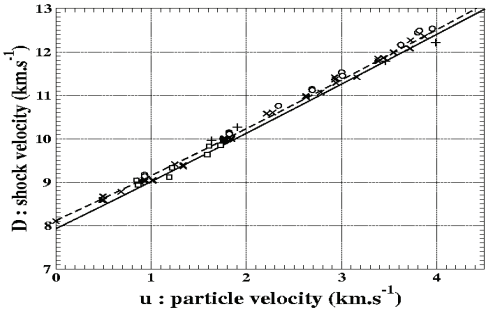

Figure 8. Calculated shock velocity D as a function of particle velocity u compared with SESAME EOS and various experimental data (see text).

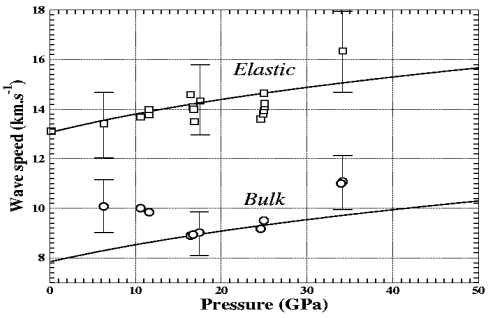

Figure 9. Calculated wave speeds (full lines) compared with the experimental values (symbols) from [26].

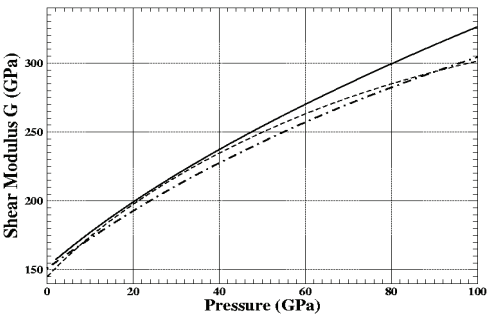

Figure 10. Calculated shear modulus under shock compared with the predictions of constitutive models: dashed line [27], dot-dashed line [17].

in Figures 6, 7 and 8 along with the predictions of the SESAME EOS (dashed line) and various experimental data : ([22], ([23], ([24], o[25].

With our assumption on the Poisson coefficient (see above), we calculated the elastic properties of beryllium at finite temperatures and pressures from our EOS. Our wave speeds calculations are compared with the experimental data of Chhabildas *et al.* [26] obtained from shock-release and shock-reshock experiments in Figure 9. We obtain a very good agreement for the elastic release wave speed but

the measured bulk velocities are higher than computed values at low pressures. As mentioned in [26], this might be due to considerable strain hardening effects. In Figure 10, we compare the evolution of the shear modulus under shock compression (full line) with the predictions of SCG [27] and Burakovsky *et al.* [17] models. Our calculations are in good agreement with both models for pressures up to 60 GPa ($T \sim 800$ K). Above this pressure range, we obtain a higher shear modulus because of a higher pressure dependence in our model. The three models having a similar temperature dependence, the difference is only due to our assumption on $\nu(\rho,T)$.

5. CONCLUSION

Using DFT, we have built a complete model in order to compute the equation of state and the elastic properties of Be at finite temperatures and pressures. This approach allows us to explain most of the unusual properties of this element, such as the decrease of the α-β transition temperature under pressure. Our calculations of the c/a ratio, the phonon spectra, and the Debye temperature are in very good agreement with available experimental data. Our equation of state successfully reproduces static and dynamic experimental data as well as previous theoretical predictions. The comparison of the calculated elastic properties of Be under shock compression with the predictions of constitutive models underlines the necessity of a better formulation for the Poisson coefficient as a function of both temperature and pressure.

References

[1] M.Y. Chou, P.K. Lam, M.L. Cohen, Phys. Rev. B 28, 4179 (1983).
[2] M. Francois and M. Contre, in Proceedings of the Conférence internationale sur la métallurgie du béryllium, Grenoble, (Presses Universitaires de France, Paris, 1965), p.201.
[3] L.C. Ming and M.H. Manghnani, J. Phys. F: Metal Phys. 14, L1 (1984).
[4] K. Nakano, Y. Akahama, H. Kawamura, J. Phys.: Condens. Matter. 14, 10569 (2002).
[5] W.J. Evans et al., Phys. Rev. B 72, 094113 (2005).
[6] P.K. Lam, M.Y. Chou, M.L. Cohen, J. Phys. C: Solid State Phys. 17, 2065 (1984).
[7] G.V. Sin'ko and N.A. Smirnov, Phys. Rev. B 71, 214108 (2005).
[8] American Institute of Physics Handbook, 3rd edn. (McGraw-Hill, New-York, 1972).
[9] O. Hunderi and H.P. Myers, J. Phys. F: Metal Phys. 4, 1088 (1974).
[10] G. Robert, to be published.
[11] J.P. Perdew et al., Phys. Rev. B 46, 6671 (1992).
[12] G. Kresse and D. Joubert, Phys. Rev. B 59, 1758 (1999).
[13] X. Gonze et al., Comput. Mater. Sci. 25, 478 (2002) ; see also http://www.abinit.org.
[14] S. Goedecker, M. Teter, R.J. Hemley, Phys. Rev. B 53, 1703 (1996).
[15] U. Haüssermann and S.I. Simak, Phys. Rev. B 64, 245114 (2001).
[16] G. Steine-Neumann and R.E. Cohen, J. Phys.: Condens. Matter 16, 8783 (2004).
[17] L. Burakovsky, C.W. Greeff and D. L. Preston, Phys. Rev. B 67, 094107 (2003).
[18] G. Grimvall, Themophysical properties of materials, (North Holland, Amsterdam, 1999).
[19] A. Migliori, H.Ledbetter, D.J. Thoma and T.W. Darling, J. Appl. Phys. 95, 2436 (2004).
[20] R. Stedman, Z. Amilius, R. Pauli and O. Sundin, J. Phys. F: Metal Phys. 6,157 (1976).
[21] K.S. Holian, Los Alamos National Laboratory Report LA-10160-MS UC-34 (1984).
[22] W.H. Isbell, F.H. Shipman and A.H. Jones, General Motors Corp. Report MSL-68-13, 1968.
[23] S.P. Marsh, LASL Shock Hugoniot Data, (University of California Press, Berkeley, 1980).
[24] J.M. Walsh, M.H. Rice, R.G. McQueen, and F.L.Yarger, Phys. Rev. 108, 196 (1957).
[25] R.G. McQueen and S.P. Marsh, Los Alamos Scientific Laboratory Report GMX-6-566 (1964).
[26] L.C. Chhabildas, J.L. Wise and J.R. Asay, in Shock Waves in Condensed Matter-1981, edited by W.J. Nellis, L. Seaman, R.A. Graham, (AIP, New York, 1982), p.422.
[27] D.J. Steinberg, S.G. Cochran, M.W. Guinan, J. Appl. Phys. 51, 1498 (1980).